ELECTROSPINNING OF ANTIBACTERIAL CELLULOSE ACETATE NANOFIBERS

İREM YAĞMUR MOL,[*] FUNDA CENGIZ ÇALLIOĞLU,[*] HÜLYA KESICI GÜLER,[*] EMEL SESLI ÇETIN[**] and GÖKSEL BILIR[**]

[*]*Textile Engineering Department, Süleyman Demirel University, Isparta, Turkey*
[**]*Medical Microbiology Department, Süleyman Demirel University, Isparta, Turkey*
✉ *Corresponding author: H. Kesici Güler, hulyakesici@sdu.edu.tr*

Received August 7, 2022

Herein, it was aimed to achieve antibacterial cellulose acetate (CA) nanofiber production and characterization. Firstly, solution properties, such as viscosity, conductivity and surface tension, were determined. Secondly, CA/zinc oxide (ZnO) composite nanofibers were produced with optimum process parameters via the electrospinning method. Then, the electrospun nanofibers were characterized by SEM, EDX, DSC, TGA, XRD, air permeability and water vapor permeability testing. Lastly, antibacterial activity tests were carried out in accordance with the AATCC100 method, against *Staphylococcus aureus* (ATCC 25923) and *Escherichia coli* (ATCC 25922).
According to the results, solution conductivity decreased and surface tension did not change with ZnO concentration. On the other hand, viscosity decreased significantly with the first addition of ZnO and then increased slightly with increasing ZnO concentration. Generally, fine (354–464 nm), uniform and beadless nanofibers were obtained. Average fiber diameter, air permeability and water vapor permeability increased with ZnO concentration. EDX analysis results verified the existence of ZnO in the structure of CA nanofibers. As a result of antibacterial studies, it was determined that the CA/zinc oxide (ZnO) composite nanofibers with the highest concentration of ZnO showed very good antibacterial activity against both *S. aureus* and *E. coli* bacterial strains.

Keywords: cellulose acetate, zinc oxide, electrospinning, antibacterial nanofibers

INTRODUCTION

Handling and utilizing nanoparticles have attracted much interest in various application areas during the past few years. Among the numerous approaches to enhancing their applicability, particle immobilization on support matrices has been investigated.[1,2] However, most applications use metal oxide nanoparticles, such as ZnO, only once, which might cause an environmental hazard, if they are not properly disposed of after usage. Nanoparticles can be supported by meshes or composites to minimize their ecological impact. Therefore, without diminishing their characteristics, immobilization provides long-term use, including reusability and recycling. Electrospinning is the most commonly utilized immobilization method, as electrospun nanofibers may easily incorporate nanoparticles.[3,4]

Due to its widespread use, cellulose, as well as its derivatives, is often regarded as the safest and most acceptable group of polymers for use in bio-applications. Cellulose is one of the most naturally abundant semi-crystalline biopolymers, and has biodegradability, biocompatibility, thermal stability, good hydrophilicity, very good moisture management, and chemical resistance properties, which are widely sought after in a wide range of biomedical applications, including wound dressings and antimicrobial uses. Additionally, its smoothness, low cost, non-toxicity, and environmental friendliness are some of its other appreciated features.[5-9] Cellulose acetate is mostly used for the development of products with various kinds of surfaces, for example, fibers,[10] membranes,[11] or films.[12] The use of electrospun cellulose acetate nanofibers as antibacterial drug carriers and wound dressing has been the focus of numerous recent studies.[13-15] Majumder *et al*. produced silver nanoparticles loaded into cellulose acetate/polyethylene glycol nanofibers by electrospinning. They performed antibacterial analysis, quantitatively evaluating

the colony forming units of *E. coli* (strain 231-b) and *S. aureus* (strain RM_AST_SA012) bacterial strains. According to the results of their antibacterial analysis, cellulose acetate/polyethylene glycol nanofibrous surfaces showed satisfactory antibacterial efficacy against *E. coli* and *S. aureus*. The authors concluded that these antibacterial nanofibers have potential application in wound dressings.[16] Nthunya and his research group investigated β-cyclodextrin/cellulose acetate nanofibers embedded with silver and silver/iron nanoparticles *via* a benign process involving *in situ* electrospinning for the removal of bacteria from water. Antibacterial analysis was carried out by minimum inhibitory concentration (MIC) tests against 12 bacterial strains. The researchers determined that silver and silver/iron nanoparticles embedded in the β-cyclodextrin/cellulose acetate nanofibers exhibited a strong biocidal effect on all the bacterial strains, which makes them ideal for antibacterial purification of water.[17]

Bacterial infection has long been recognized as a trying circumstance that has affected humans. With the evolution of antibacterial compounds, high-tech textile products with antibacterial properties have gained worldwide attention in recent years and are widely considered an effective method of bacterial infection reduction.[1,18,19] Electrospun webs are excellent materials for protecting against harmful microbes due to their very small fiber diameter (nm), high porosity, high specific surface area (m^2/g), and small pore size. The excellent fit of electrospun mats means that they can be used as incredibly effective delivery platforms for bioactive compounds such as antimicrobials. These agents are most often integrated into electrospun materials *via* a variety of different techniques, depending on the agents and application areas.[5,20,21]

While some nanoparticles are extremely hazardous, such as CdO (cadmium oxide), others, such as ZnO, AgO (silver (II) oxide), and TiO_2 (titanium dioxide), are non-toxic and are utilized in a wide range of commercial products.[22] ZnO is a UV sensitive catalyst that has low toxicity and high thermal and chemical stability properties. It offers a wide range of potential applications, including in antibacterial, anticancer, antifungal, antidiabetic, anti-inflammatory, wound healing, and antioxidant materials, as well as drug delivery and bio-imaging applications.[3,23-27] Additionally, it has been utilized in the cosmetics sector, agriculture, and in the production of electrical devices; also, due to its contribution to fibroblast proliferation and angiogenesis, it is utilized as an active component in wound dressings.[28-31] Numerous processes, including pulsed laser deposition,[32] sol–gel,[33,34] metal-organic chemical vapor deposition,[35] thermal evaporation,[36] and spray pyrolysis,[37] have been used to obtain structures containing ZnO. A typical strategy to improve its performance is to use nanostructured ZnO. Due to the easy operation and high loading capacity of electrospinning, nanofiber structures have been produced using this technique.[27,38]

Thus, in the present research, a CA/ZnO nanofibrous material will be produced, which is intended to achieve high air permeability, water vapor permeability and antibacterial activity (in accordance with AATCC100 standards). This nanofibrous material is intended to be used as an antibacterial interface in disposable masks.

EXPERIMENTAL

Material

In this study, CA (30.000 g/mol) was used as a polymer, DMAC and acetone were used as solvents, ZnO nanoparticles (500 nm) were used as an antibacterial agent, Phosphate Buffer Saline (PBS, pH 7.4) was used as medium for antibacterial analyses. CA polymer and PBS were purchased by Sigma Aldrich Company, DMAC was supplied by Fluka, acetone was provided from ISOLAB, and ZnO antibacterial agent was obtained from Merck.

During the polymer solution preparations, a 16 wt% CA polymer concentration was applied. The antibacterial agent was used at 0, 0.2, 0.4, 0.6, 0.8, and 1 wt% concentrations. All the solutions were prepared under the same conditions, such as stirring time, stirring speed (rpm), temperature, *etc*. (Table 1).

Polymer solution properties

Firstly, solvent optimization studies were achieved with DMAC and acetone, and the optimum DMAC:acetone ratio was obtained as 1:2. Then, CA/DMAC:acetone solutions were prepared at 16 wt% concentration of CA, with various ZnO concentrations. Then, polymer solution properties, such as viscosity (SOIF NDJ-8S) under the shear rate of 3 s^{-1}, conductivity (Selecta CD 2005) and surface tension (Biolin Scintific Sigma 702), by the Wilhelmy Plate method, were determined.

Electrospinning process

Nanofiber production was achieved by conventional laboratory scale electrospinning. During the spinning process, 22 kV voltage (Matsusada Precision Inc. Power Supply), 0.2 mL/h solution feed

rate (New Era Pump Systems), and 21 cm distance between the electrodes were applied for all the solutions. Furthermore, all the samples were electrospun under ambient conditions of 27% ±1 humidity and 22.7 °C ±1 temperature (Table 2). All the nanofibers were produced in an hour and collected on aluminum foil.

Table 1
CA/DMAC:acetone polymer solutions with various ZnO concentrations

Polymer solution codes	Polymer concentration (wt%)	DMAC/acetone ratio (wt%)	ZnO concentration (wt%)
CA0	16	1:2	0
CA0.2	16	1:2	0.2
CA0.4	16	1:2	0.4
CA0.6	16	1:2	0.6
CA0.8	16	1:2	0.8
CA1	16	1:2	1

Table 2
Process parameters of electrospinning

Voltage (kV)	Distance between electrodes (cm)	Feed rate (mL/h)	Humidity (%)	Temperature (°C)	Needle diameter (mm)
22	21	0.2	27	22.7	0.8

Characterization of electrospun nanofibers

Fiber morphology analysis

The morphology of electrospun CA nanofibers was analyzed with a FEI Quanta 250 FEG Scanning Electron Microscope (SEM). Fiber diameters were measured with Image J software. Then, the fiber diameter uniformity coefficient was calculated with a method that uses the same principle as for molar mass distribution in chemistry science.[39] The number average and weight average values were calculated using Equations (1) and (2) given below:

$$A_n = \frac{\sum n_i d_i}{\sum n_i} \text{ (number average)} \quad (1)$$

$$A_w = \frac{\sum n_i d_i^2}{\sum n_i d_i} \text{ (weight average)} \quad (2)$$

where d_i – fiber diameter, n_i – fiber number.

The fiber diameter uniformity coefficient was determined by the ratio A_w/A_n. An ideal optimum value should be close to 1 for uniform fibers. Fiber diameter histogram curves were obtained using the SPSS statistical program.

EDX spectroscopy

Energy dispersive X-ray (EDX) spectroscopy was achieved to confirm the existence of ZnO in the CA nanofibers with a FEI Quanta 250 FEG device.

TGA analysis

Thermogravimetric analysis (TGA) was performed with an Exstar SII TG DTA 7200 to determine the thermal stability of CA powder, CA1 and CA6 nanofibers in a nitrogen gas environment, by gradually increasing the temperature from room temperature to 600 °C, at a rate of 10 °C per minute.

DSC analysis

Differential scanning calorimetry (DSC) analysis was performed using a Perkin Elmer DSC 4000 to determine the glass transition, melting and decomposition temperatures, and enthalpies of ZnO, CA powder, CA0 and CA6 nanofibers in a nitrogen gas environment from 24 °C to 600 °C, with a 10 °C/min temperature increase.

XRD analysis

XRD measurements were performed to investigate the integration of the ZnO nanoparticles into the nanofibrous membranes. The measurements were recorded with a Bruker D8 Twin device in the range of 2Θ: 5-60º.

Air and water vapor permeability

Air permeability and water vapor permeability were measured for all CA solution samples. Air permeability was determined according to EN-ISO 9237 and water vapor permeability was specified according to BS 7209 and BS 3424 standards.

Antibacterial activity

Lastly, antibacterial analyses were carried out by the AATCC100 method. Briefly, bacterial suspensions were adjusted to 0.5 McFarland. All nanofiber mats were cut to 1 cm x 1 cm dimensions. Then, 100 µL of bacterial suspension was added to the nanofiber samples and vortexed. For zero-time analysis, 1 mL of PBS was added, and 10-fold dilutions of this solution were prepared up to 10^{-11}. A sample of 10 µL from each dilution was spread onto Columbia agar (Becton Dickinson) plates, and then incubated aerobically for 24 h at 35 ± 2 °C. For 18 hours analyses, after adding

100 µL of bacterial suspension to the nanofiber samples, the samples were incubated at 35 ± 2 °C for 18 hours. Then, 1 mL of PBS was added, and 10-fold dilutions of this solution were prepared up to 10^{-11}. A sample of 10 µL from each dilution was spread onto Columbia agar (with 5% sheep blood) plates, and then incubated aerobically for 24 h at 35 ± 2 °C. Lastly, bacterial colonies were counted. Standard bacterial strains that are often found in textiles and skin and can be encountered in many kinds of application areas of nanofibers, such as medical applications (face masks, wound dressings *etc*.), were chosen for this study.

RESULTS AND DISCUSSION

Solution properties results

Electrospinning is a simple and efficient technique for producing fibrous materials, but the final fiber morphology is strongly influenced by the properties of the polymer solution, especially its viscosity, conductivity, and surface tension. Furthermore, the addition of nanoparticles can change these parameters; therefore, a thorough examination of these parameters for CA solutions incorporating ZnO may be important. For this purpose, solution properties, such as viscosity, conductivity and surface tension, were determined. Prior to the electrospinning process, the polymer solution conductivity is an incredibly critical characteristic to consider, especially when dealing with nanoparticle-containing solutions.[40] The properties of CA polymer solutions with various concentrations of ZnO are given in Figure 1.

According to the polymer solution conductivity results, conductivity decreased, except for CA1, as ZnO concentration increases (Fig. 1 and Table 3). In the literature, Rodriguez-Tobias and his research group studied poly(D,L-lactide) nanofibers incorporating different concentrations of ZnO nanoparticles. They determined a similar outcome as in our study that conductivity decreases with the addition of ZnO into the poly(D,L-lactide) polymer solutions. The conductivity of the poly(D,L-lactide) polymer solution diminished from 6.23 to 3.17 µS/cm by adding 1 wt% of ZnO nanoparticles. However, as the ZnO nanoparticle concentrations were increased – to 3 and 5 wt%, the conductivity also increased from 3.36 ± 0.03 to 4.41 ± 0.18 µS/cm.[41] The conductivity increases at 1% ZnO concentration, as also observed in our study. We would have probably obtained higher conductivity results, if we had continued to increase the ZnO concentration. In addition, the same tendency of conductivity values was observed as in the cited study; the difference in conductivity values is thought to be due to the difference in the polymer and solvent used. This is explained by the fact that the conductivity is not only affected by the addition of an inorganic material, but also by the polymer and solvent used.[42]

Viscosity decreased significantly at the first addition of 0.2 wt% ZnO and then increased slightly with increasing ZnO concentration. On the other hand, surface tension did not change with the variation of ZnO concentration. It is already well known from the literature that the addition of ZnO to polymer solutions does not result in a considerable increase in surface tension.[38,43]

Fiber morphology results

Fiber morphology was investigated using SEM. SEM images and fiber diameter histograms of CA/ZnO nanofibers, with various concentrations of ZnO, are given in Figure 2. It was determined that the average fiber diameter increased with a rising ZnO concentration. Overall, quite fine, uniform nanofibers and highly porous surfaces were produced. The presence of ZnO nanoparticles in the nanofibrous structure, especially in CA0.8 and CA1 samples (Fig. 2), can be clearly seen.

In this study, sample CA0.8 was determined to be the optimum in terms of fiber morphology and ZnO concentration. In addition, the fiber diameter histogram of sample CA0.8 showed the most unimodal curve and uniform size distribution. Figure 3 illustrates the average fiber diameter and fiber diameter uniformity coefficient values changing with ZnO concentration.

As mentioned above, it is clearly seen that the average fiber diameter increased with ZnO concentration. The addition of ZnO nanoparticles enhanced the charge density on the ejected jet surface during electrospinning, resulting in a considerable increase in the total electric charge carried by the electrospinning jet. An increasing number of charged nanoparticles carried by the jet resulted in higher elongation forces being applied to the jet under the effect of an electrical field, enabling it to overcome self-repulsion. In other words, although the diameter of the final nanofibers decreases much more than before, as the charge density increases, it has been found to occur in thicker nanofibers with the increase in viscosity.[29,44,45]

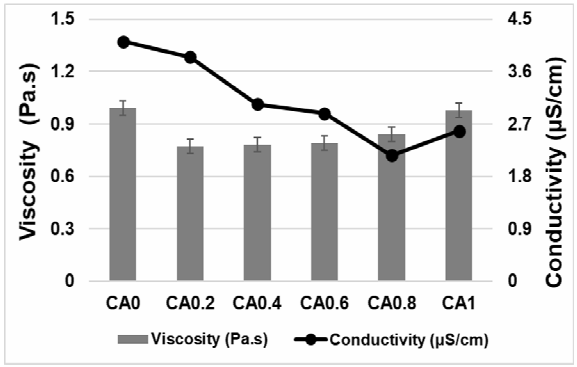

(a)

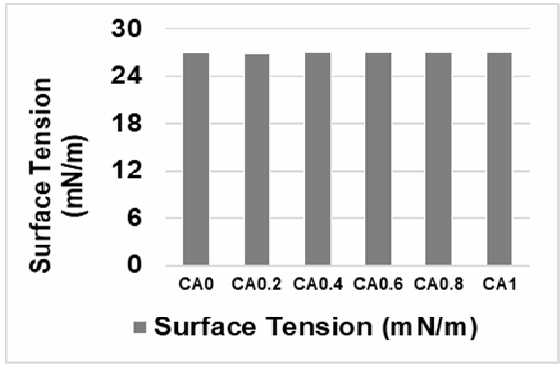

(b)

Figure 1: Solution properties results of CA/ZnO solutions, a) viscosity and conductivity, b) surface tension

Table 3
Solution and fiber properties of CA/ZnO samples

Sample codes	Conductivity (µS/cm)	Surface tension (mN/m)	Viscosity (Pa.s) (shear rate 3^{-1}s)	Weight average diameter (A_W)(nm)	Number average diameter (A_n)(nm)	Fiber diameter uniformity coefficient (A_W/A_n)	Nanoweb morphology
CA0	4.12	26.95	0.99	368.8	353.9	1.04	Smooth
CA02	3.85	26.78	0.77	436.9	411.5	1.06	Less sticky
CA04	3.04	27.04	0.78	498.7	436.9	1.14	Less sticky
CA06	2.88	27.04	0.79	484.6	441.2	1.1	Less sticky
CA08	2.16	27.11	0.84	478.5	457	1.05	Smooth
CA1	2.58	27.02	0.98	541.1	464	1.17	Smooth

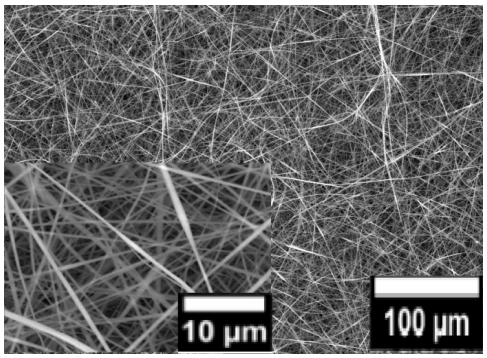

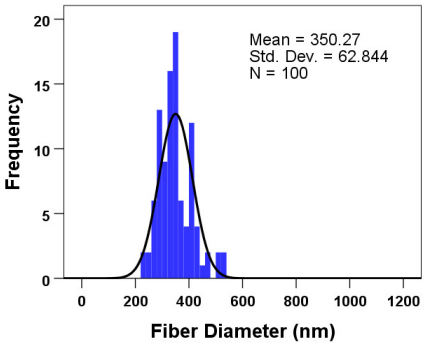

CA0

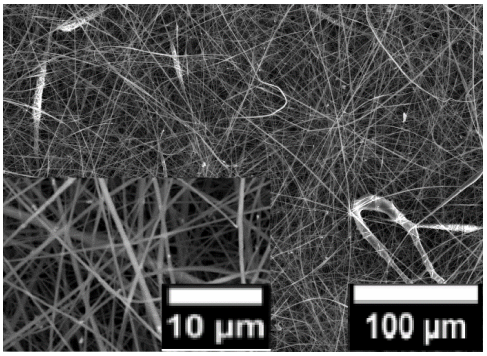

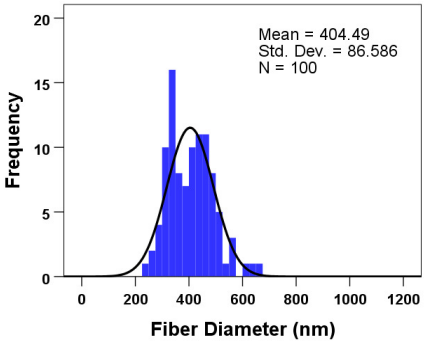

CA0.2

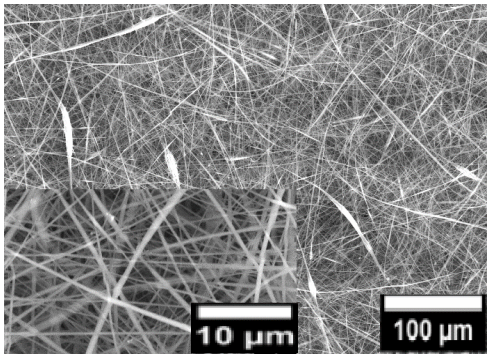

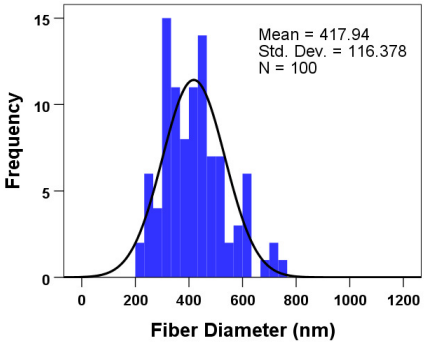

CA0.4

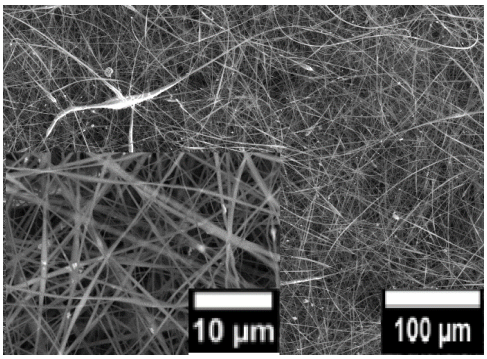

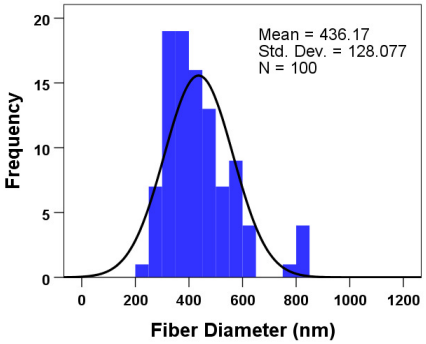

CA0.6

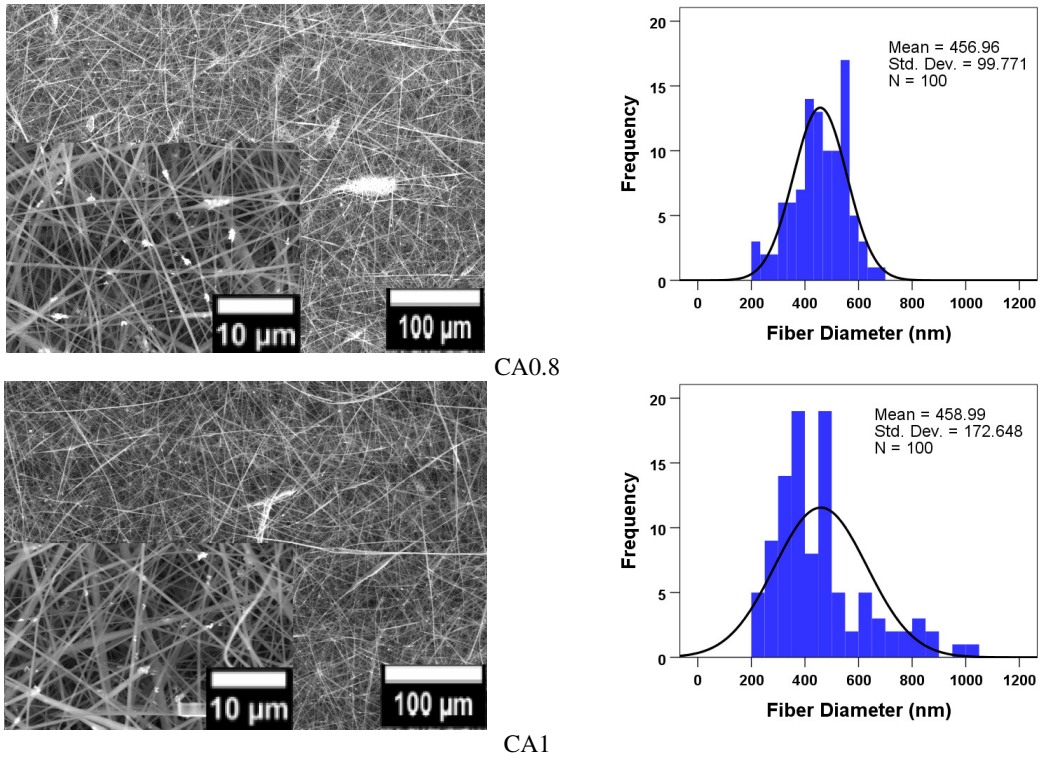

Figure 2: SEM images (1.000x-10.000x) and histograms of CA nanofibers produced with various concentrations of ZnO

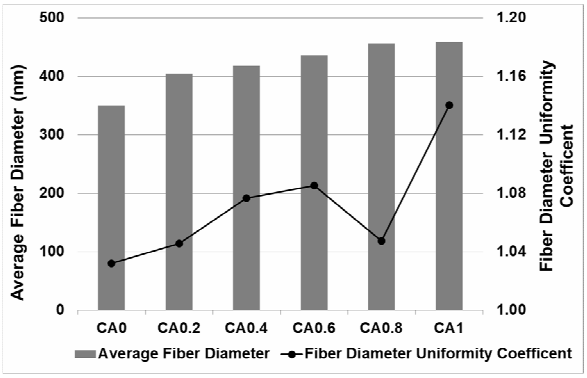

Figure 3: Average fiber diameter and diameter uniformity results of CA nanofibers with various concentrations of ZnO

This situation led to variation in nanofiber diameter distribution and thus deterioration in uniformity in histograms with increasing ZnO concentration. Thus, the most uniform nanofibers were obtained from CA0 (1.04) and CA0.8 (1.05). Also, the finest nanofibers were obtained from CA0 as a 353.9 nm. All solution properties and fiber morphology results are given in Table 3.

EDX results

The existence of ZnO nanoparticles entrapped within the CA nanofibrous webs was confirmed by the EDX spectra of CA and CA/ZnO nanocomposites. Another confirmation is that, throughout the electrospinning process, the ZnO nanoparticles reached successfully the collector together with the polymer solution. EDX spectra of pure CA nanofibers (CA0) and those incorporating various concentrations of ZnO nanoparticles are shown in Figure 4.

It is possible to say that there are no other impurities associated with the compounds, as shown by the EDX spectra. In the EDX spectrum of pure CA nanofibers, only the peaks assigned to the Kα peaks of carbon (C) and oxygen (O) were found, as expected.[46] Three characteristic peaks

were observed in the CA/ZnO composite nanofibers at the energy levels 1 keV, 8.5 keV, and 9 keV, which have the zinc element. When the spectra were examined in detail, it was observed that the intensity of the peaks corresponding to zinc at lower concentrations, such as 0.2, 0.4, and 0.6 wt%, were quite low and could not even be detected at high energy levels. However, at higher concentrations, such as 0.8% and 1%, all three characteristic peaks were determined. This is explained by the fact that minimal elements generate X-ray peaks that are difficult to distinguish from background radiation.[29] Table 4 shows the elemental analysis of Zn and O elements existing in the CA nanofibrous structure. It was observed that the amounts of ZnO increased with ZnO concentration.

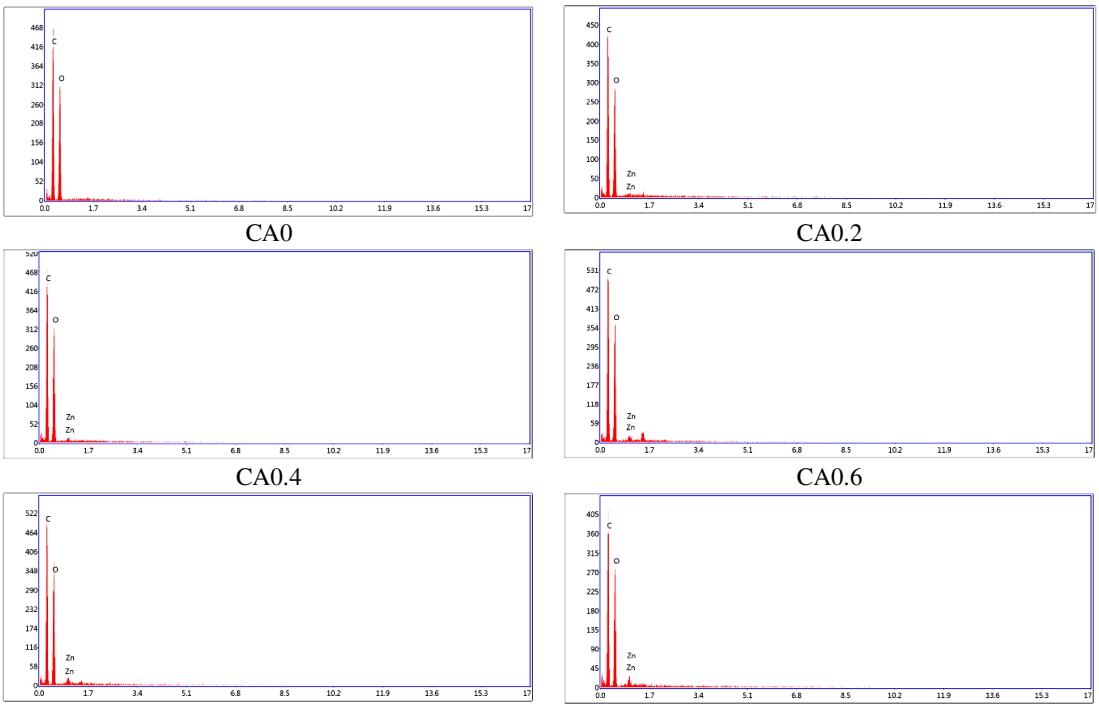

Figure 4: EDX analysis of CA solutions with various concentrations of ZnO

Table 4
SEM-EDX results of CA nanofibers with various concentrations of ZnO

Sample code	C (%)	O (%)	Zn (%)
CA0	52.98	47.02	-
CA0.2	54.02	45.27	0.72
CA0.4	54.09	44.90	1.01
CA0.6	54.11	44.37	1.52
CA0.8	52.73	44.75	2.52
CA1	53.23	43.27	3.50

Thermal analysis

TGA results

Thermal analyses were carried out to examine to effect of added ZnO nanoparticles and increased ZnO concentration on the thermal stability of CA nanofibers. Figure 5 shows the thermal behavior of CA/ZnO nanofibers. As can be seen, the main weight loss is around 240-250 °C for all the samples. As can be noted on the curve of CA1, after 375 °C, the material

containing the most ZnO left the highest residue – in a ratio of 30%. The lowest residue was obtained from CA0, in a ratio lower than 1%. According to the TGA results, it was observed that ZnO addition increased the thermal resistance of the material

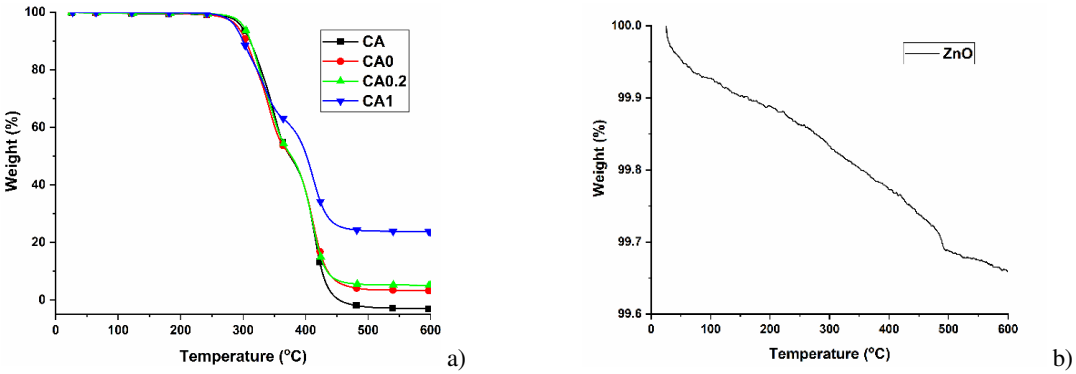

Figure 5: TGA thermograms of a) CA powder, CA0, CA0.2 and CA1 nanofibers, b) ZnO

DSC results

The DSC curves of ZnO, CA polymer, CA0, and CA1 nanofibers are given in Figure 6. Generally, the temperature at which the fibers begin to degrade is between 225 °C and 230 °C; and final degradation temperatures are between 220 °C and 250 °C. The first peak, which is the glass transition temperature, decreased in the CA1 sample due to the addition of ZnO.

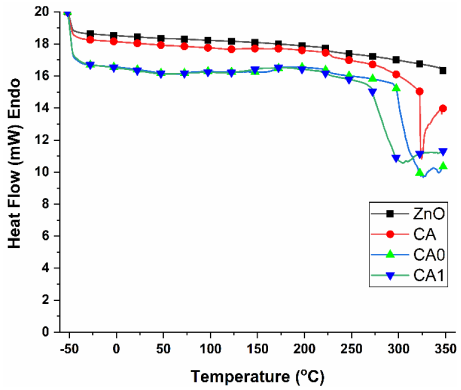

Figure 6: DSC curves of ZnO, CA polymer, CA0 and CA1 nanofibers

XRD results

To determine whether the prepared material was crystalline or amorphous, XRD analysis was performed. Figure 7 shows the XRD diffractograms of ZnO, CA powder, CA0 nanofibers and CA1 nanofibers.

It is expected that CA powder and CA0 (pure CA) nanofibers exhibit highly amorphous structure.[46] Pure ZnO shows sharp diffraction peaks at 2θ = 31.83°, 34.48°, 36.30°, 47.58°, and 56.61°.[24] Sharp diffraction peaks indicate that ZnO nanoparticles are highly crystalline.[47] When the CA1 diffractogram is analyzed, it is seen that both the amorphous structure of CA nanofibers and the characteristic peaks of ZnO nanoparticles are present. It is also clearly noted that the intensity of the peaks significantly decreased in the diffractogram of CA1, compared to that of ZnO. This is explained by the much smaller amount of ZnO nanoparticles present CA1 material (1%), compared to the diffractogram made for 100% ZnO nanoparticles. The formation of a new covalent bond between ZnO nanoparticles and CA nanofibers resulted in the appearance of characteristic ZnO peaks in the CA1 diffractogram.[28]

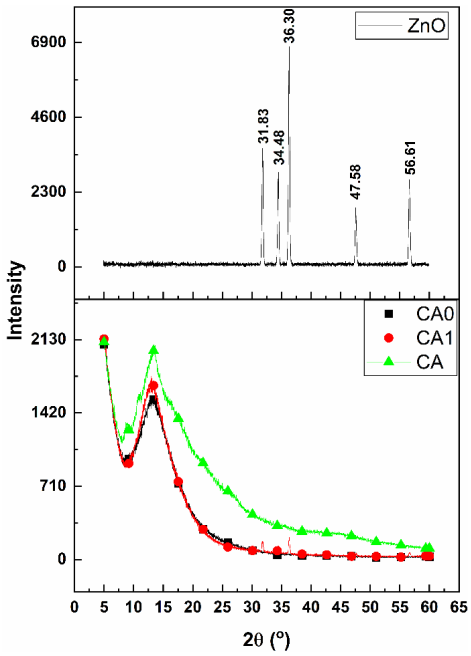

Figure 7: XRD diffractograms of ZnO, CA powder, CA0 nanofibers and CA1 nanofibers

Air and water vapor permeability results

The air and water vapor permeability values are important parameters of electrospun nanofiber mats that make them suitable for many applications.[48] One of the benefits of electrospinning as a membrane preparation method is that it allows fiber structure control, thus yielding the desired proerties.[32] The results of air permeability and water vapor permeability of CA nanofibers with various concentrations of ZnO are given in Figure 8. It is obviously seen that water vapor permeability and air permeability showed a remarkably increasing tendency with rising ZnO concentration. It is well known from the literature that the average pore size increases as the average fiber diameter increases in nanofibers. Specifically, air permeability is directly related to porosity and fiber diameter. Therefore, a larger pore diameter will result in larger diffusion channels for air and water vapor permeability.[49] This trend could be attributable to the pore size and average fiber diameter of the nanofibrous material, the smaller the average pore size, the greater air resistance.[50]

Antibacterial activity results

Antibacterial activity results are given in Figures 9 and 10 for *S. aureus* and *E. coli*, respectively. It is clearly seen from the images that ZnO had significant antibacterial activity against *S. aureus*. More precisely, CA0 and CA0.8 did not show antibacterial activity at zero time. It is possible to say that ZnO has no effect at zero time. Similarly, as expected, antibacterial activity was not detected in the control sample CA0, either at zero time or after 18 hours. However, there is quite a difference between zero time and 18 hours Petri dishes for CA0.8. For the CA0.8 sample, while the bacterial colonies are observed up to the 7^{th} dilution at zero time, there is only the presence of bacteria until the 3^{rd} dilution at the end of 18 hours.

As regards the behaviour of the materials towards *E. coli*, the results were similar to those regarding *S. aureus*. As expected, no antibacterial activity was observed in the control sample CA0. In addition, no antibacterial activity was observed in the CA0.8 sample at zero time, similarly to the CA0 sample. There were a lot fewer bacterial colonies in the CA0.8 sample than in the other samples after 18 hours. This is an indication that ZnO has an effect against *E. coli* bacteria colonies. Table 5 presents the number of *E. coli* and *S. aureus* bacterial colonies for CA without and with ZnO. According to the quantitative data obtained indicating the numbers of bacterial colonies, it can be concluded that the exposure to the material containing ZnO induced a reduction of 10^3 of both *S. aureus* and *E. coli* bacterial colonies after 18 hours.

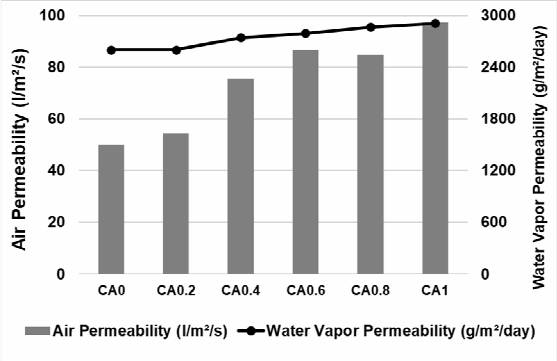

Figure 8: Air permeability and water vapor permeability of CA nanofibers with various concentrations of ZnO

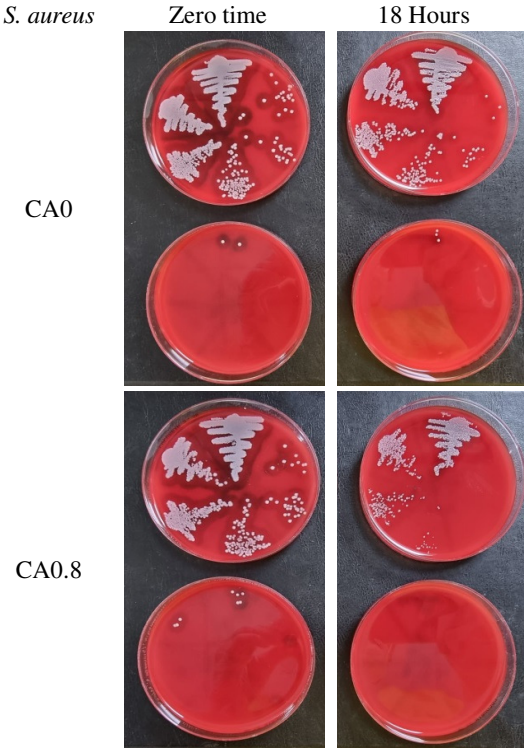

Figure 9: Antibacterial activity of CA without and with 0.8 wt% ZnO nanofibers against *S. aureus*

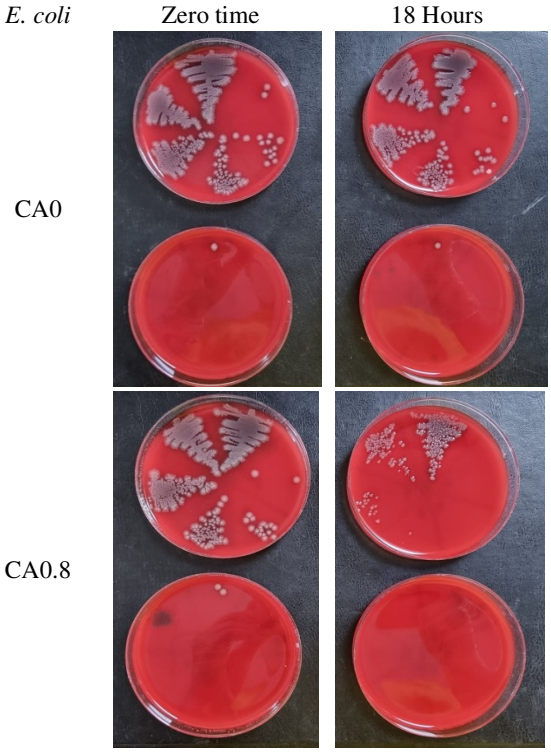

Figure 10: Antibacterial activity of CA without and with 0.8 wt% ZnO nanofibers against *E. coli*

Table 5
Number of bacterial colonies for CA without and with ZnO

Bacteria	Time	Sample	Number of bacterial colonies
E. coli	Zero time	CA0.8	10^8
		CA0	10^8
	18 hours	CA0.8	10^5
		CA0	10^9
S. aureus	Zero time	CA0.8	10^8
		CA0	10^8
	18 hours	CA0.8	10^5
		CA0	10^9

CONCLUSION

In the present study, antibacterial CA nanofibers were produced by the electrospinning method with various ZnO concentrations, namely 0, 0.2, 0.4, 0.6, 0.8, and 1 wt%. The materials obtained were characterized by SEM, EDX and TGA, as well as in terms of solution properties, air permeability, water vapor permeability, and antibacterial activity against *S. aureus* and *E. coli* bacteria. The results indicated that solution conductivity decreased and surface tension did not change with ZnO concentration, while viscosity decreased significantly at the first addition of ZnO and then increased slightly with rising ZnO concentration. Generally, fine (354–464 nm), uniform, and beadless nanofibers were obtained. Average fiber diameter, air permeability, and water vapor permeability increased with ZnO concentration. EDX analysis results verified the existence of ZnO in the structure of CA nanofibers. Antibacterial activity results demonstrated that CA nanofibers incorporating 0.8 wt% ZnO have excellent antibacterial properties, compared to pure CA nanofibers.

The findings of this study demonstrate that the developed CA/ZnO composite nano-material exhibits high antibacterial activity, as well as high air and water vapor permeability, suggesting that it can be useful in biomedical applications, such as disposable masks and wound dressings.

ACKNOWLEDGEMENTS: The authors would like to express appreciation for the financial support of the Süleyman Demirel University, Scientific Research Project Unit [Project Number: FYL-2020-8206]; and to the Scientific and Technological Research Council of Turkey for their support of the 2247-C Trainee Researcher Scholarship Program (STAR) 2020/1.

REFERENCES

[1] Y. Jia, G. Huang, F. Dong, Q. Liu and W. Nie, *Polym. Compos.*, **37**, 2847 (2016), https://doi.org/10.1002/pc.23481

[2] S. Wang, L. Sun, B. Zhang, C. Wang, Z. Li *et al*., *Polym. Compos.*, **32**, 347 (2011), https://doi.org/10.1002/pc.21038

[3] M. L. A. Anero, A. D. S. Montallana and M. R. Vasquez Jr., *Results Phys.*, **25**, 104223 (2021), https://doi.org/10.1016/j.rinp.2021.104223

[4] A. D. S. Montallana, B.-Z. Lai, J. P. Chu and M. R. Vasquez Jr., *Mater. Today Commun.*, **24**, 101183 (2020), https://doi.org/10.1016/j.mtcomm.2020.101183

[5] T. Czapka, A. Winkler, I. Maliszewska and R. Kacprzyk, *Energies*, **14**, 2598 (2021), https://doi.org/10.3390/en14092598

[6] M. T. Elsayed, A. A. Hassan, S. A. Abdelaal, M. M. Taher, M. Khalaf Ahmed *et al*., *J. Mater. Res. Technol.*, **9**, 13927 (2020), https://doi.org/10.1016/j.jmrt.2020.09.094

[7] A. W. Jatoi, I. S. Kim and Q.-Q. Ni, *Carbohyd. Polym.*, **207**, 640 (2019), https://doi.org/10.1016/j.carbpol.2018.12.029

[8] K. Kalwar and M. Shen, *Nanotechnol. Rev.*, **8**, 246 (2019), https://doi.org/10.1515/ntrev-2019-0023

[9] M. Q. Khan, D. Kharaghani, A. Shahzad, Y. Saito, T. Yamamoto *et al*., *Polym. Test.*, **74**, 39 (2019), https://doi.org/10.1016/j.polymertesting.2018.12.015

[10] K. Khoshnevisan, H. Maleki, H. Samadian, S. Shahsavari, M. H. Sarrafzadeh *et al*., *Carbohyd. Polym.*, **198**, 131 (2018), https://doi.org/10.1016/j.carbpol.2018.06.072

[11] R. K. Mishra, P. Mishra, K. Verma, A. Mondal, R. G. Chaudhary *et al*., *Environ. Chem. Lett.*, **17**, 767 (2019), https://doi.org/10.1007/s10311-018-00838-w

[12] V. Gomes, A. S. Pires, N. Mateus, V. de Freitas and L. Cruz, *Food Hydrocolloid*, **127**, 107501 (2022), https://doi.org/10.1016/j.foodhyd.2022.107501

[13] R. E. Demirdogen, *Cellulose Chem. Technol.*, **56**, 559 (2022), https://doi.org/10.35812/CelluloseChemTechnol.2022.56.48

[14] L. Lei, W. Huang, K. Liu, X. Liu, M. Dai *et al*., *J. Drug. Deliv. Sci. Tec.*, **69**, 102863 (2022), https://doi.org/10.1016/j.jddst.2021.102863

[15] M. A. Wsoo, S. Shahir, S. P. M. Bohari, N. H. M. Nayan and S. I. Abd Razak, *Carbohyd. Res.*, **491**, 107978 (2020), https://doi.org/10.1016/j.carres.2020.107978

[16] S. Majumder, M. A. Matin, A. Sharif and M. T. Arafat, *J. Polym. Res.*, **27**, 1 (2020), https://doi.org/10.1007/s10965-020-02356-2

[17] L. N. Nthunya, M. L. Masheane, S. P. Malinga, E. N. Nxumalo, T. G. Barnard *et al*., *ACS Sustain. Chem. Eng.*, **5**, 153 (2017), https://doi.org/10.1021/acssuschemeng.6b01089

[18] A. Abramova, A. Gedanken, V. Popov, E.-H. Ooi, T. J. Mason *et al*., *Mater. Lett.*, **96**, 121 (2013), https://doi.org/10.1016/j.matlet.2013.01.041

[19] J. Zhu, Z. Ge and Z. Song, *IFAC Journal of Systems and Control*, **6**, 1 (2018), https://doi.org/10.1016/j.ifacsc.2018.09.002

[20] F. C. Çallıoğlu, H. K. Güler and E. S. Çetin, *Mater. Res. Express.*, **6**, 125013 (2019), https://doi.org/10.1088/2053-1591/ab5387

[21] H. Jiang, L. Wang and K. Zhu, *J. Control. Release*, **193**, 296 (2014), https://doi.org/10.1016/j.jconrel.2014.04.025

[22] A. Wiesenthal, L. Hunter, S. Wang, J. Wickliffe and M. Wilkerson, *Int. J. Dermatol.*, **50**, 247 (2011), https://doi.org/10.1111/j.1365-4632.2010.04815.x

[23] H. Agarwal, S. V. Kumar and S. Rajeshkumar, *Resource-Efficient Techn*., **3**, 406 (2017), https://doi.org/10.1016/j.reffit.2017.03.002
[24] R. J. B. Butalid, A. P. S. Cristobal, A. D. S. Montallana and M. R. Vasquez Jr., *J. Vac. Sci. Techn. B*, **38**, 062205 (2020), https://doi.org/10.1116/6.0000306
[25] B. İkizler and S. M. Peker, *Thin Solid Films*, **605**, 232 (2016), https://doi.org/10.1016/j.tsf.2015.11.083
[26] J. Jiang, J. Pi and J. Cai, *Bioinorg. Chem. Appl*., **2018**, 1062562 (2018), https://doi.org/10.1155/2018/1062562
[27] W. Wang, H. Huang, Z. Li, H. Zhang, Y. Wang *et al*., *J. Am. Ceram. Soc*., **91**, 3817 (2008), https://doi.org/10.1111/j.1551-2916.2008.02765.x
[28] R. Ahmed, M. Tariq, I. Ali, R. Asghar, P. N. Khanam *et al*., *Int. J. Biol. Macromol*., **120**, 385 (2018), https://doi.org/10.1016/j.ijbiomac.2018.08.057
[29] R. Augustine, H. N. Malik, D. K. Singhal, A. Mukherjee, D. Malakar *et al*., *J. Polym. Res*., **21**, 1 (2014), https://doi.org/10.1007/s10965-013-0347-6
[30] M. Imran, S. Haider, K. Ahmad, A. Mahmood and W. A. Al-Masry, *Arab. J. Chem*., **10**, S1067 (2017), https://doi.org/10.1016/j.arabjc.2013.01.013
[31] A. Naveed Ul Haq, A. Nadhman, I. Ullah, G. Mustafa, M. Yasinzai *et al*., *J. Nanomater*., **2017**, 1 (2017), https://doi.org/10.1155/2017/8510342
[32] D. Zhang and D. Brodie, *Thin Solid Films*, **238**, 95 (1994), https://doi.org/10.1016/0040-6090(94)90655-6
[33] M. Kamalasanan and S. Chandra, *Thin Solid Films*, **288**, 112 (1996), https://doi.org/10.1016/S0040-6090(96)08864-5
[34] M. Ohyama, H. Kouzuka and T. Yoko, *Thin Solid Films*, **306**, 78 (1997), https://doi.org/10.1016/S0040-6090(97)00231-9
[35] W. I. Park, D. H. Kim, S.-W. Jung and G.-C. Yi, *Appl. Phys. Lett*., **80**, 4232 (2002), https://doi.org/10.1063/1.1482800
[36] P. Gao and Z. L. Wang, *J. Phys. Chem. B*, **106**, 12653 (2002), https://doi.org/10.1021/jp0265485
[37] L. Bahadur, M. Hamdani, J. Koenig and P. Chartier, *Sol. Energ. Mater*., **14**, 107 (1986), https://doi.org/10.1016/0165-1633(86)90069-9
[38] D. Y. Lee, J.-E. Cho, N.-I. Cho, M.-H. Lee, S.-J. Lee *et al*., *Thin Solid Films*, **517**, 1262 (2008), https://doi.org/10.1016/j.tsf.2008.05.027
[39] F. Cengiz and O. Jirsak, *Fiber. Polym*., **10**, 177 (2009), https://doi.org/10.1007/s12221-009-0177-7
[40] N. Bhardwaj and S. C. Kundu, *Biotechnol. Adv*., **28**, 325 (2010), https://doi.org/10.1016/j.biotechadv.2010.01.004
[41] H. Rodríguez-Tobías, G. Morales, A. Ledezma, J. Romero and D. Grande, *J. Mater. Sci*., **49**, 8373 (2014), https://doi.org/10.1007/s10853-014-8547-y
[42] W. A. Sarhan, H. M. Azzazy and I. M. El-Sherbiny, *Mater. Sci. Eng. C*, **67**, 276 (2016), https://doi.org/10.1016/j.msec.2016.05.006
[43] N. A. Elgheryani, *Iraq. J. Phys*., **17**, 119 (2019), https://doi.org/10.30723/ijp.v17i40.412
[44] G. Ma, D. Yang and J. Nie, *Polym. Adv. Technol*., **20**, 147 (2009), https://doi.org/10.1002/pat.1180
[45] X. Zong, K. Kim, D. Fang, S. Ran, B. S. Hsiao *et al*., *Polymer*, **43**, 4403 (2002), https://doi.org/10.1016/S0032-3861(02)00275-6
[46] S. Ahmadian-Fard-Fini, D. Ghanbari, O. Amiri and M. Salavati-Niasari, *Carbohyd. Polym*., **229**, 115428 (2020), https://doi.org/10.1016/j.carbpol.2019.115428
[47] Y. Gutha, J. L. Pathak, W. Zhang, Y. Zhang and X. Jiao, *Int. J. Biol. Macromol*., **103**, 234 (2017), https://doi.org/10.1016/j.ijbiomac.2017.05.020
[48] P. Gibson, *Text. Res. J*., **63**, 749 (1993), https://doi.org/10.1177/004051759306301208
[49] J. McCann and D. Bryson, "Textile-Led Design for the Active Ageing Population", Elsevier, 2014, pp. 551
[50] Z. Mao, J. Bai, X. Jin, W. Mao and Y. Dong, *Colloid. Surface B*, **208**, 112070 (2021), https://doi.org/10.1016/j.colsurfb.2021.112070